Potential Pitfalls in Imaging of the Mediastinum

Orly Goitein, MD[a,*], Mylene T. Truong, MD[b], Elena Bekker, MD[a,c], Edith M. Marom, MD[c]

KEYWORDS

• Thoracic • Mediastinum • CT • MR imaging • Pitfalls

KEY POINTS

- Advances in computed tomography technology allow visualization of normal anatomic structures and variants in greater detail, which can be misinterpreted as pathology.
- If a mediastinal mass is suspected to be cystic, MR imaging adds value by demonstrating its fluid content and is helpful to differentiate benign from malignant disease.
- An awareness of the spectrum of the potential pitfalls of mediastinal imaging and artifacts related to flow, motion, and cardiac pulsations is important for accurate interpretation.
- Flow artifacts can be resolved by obtaining a delayed venous scan.
- Artifacts owing to cardiac motion can be mitigated by using electrocardiographic gating.

INTRODUCTION

A computed tomography (CT) scan of the chest is the modality of choice for evaluating many suspected or known thoracic abnormalities involving the lungs and mediastinum. CT scans are widely available with a relatively quick acquisition time and allows for accurate and reproducible images of the mediastinum, its contents, and any associated abnormalities. Advances in multidetector CT technology, with improved temporal and spatial resolution, allow for better delineation of mediastinal structures. However, the high resolution of a CT scan also results in the routine visualization of normal anatomic structures and anatomic variants, which can be confused with pathology, as well as benign lesions that may mimic malignant neoplasms.

A CT scan may be performed for a variety of clinical scenarios, both in the acute and ambulatory settings.[1] Ideally, the CT protocol is optimized and tailored to answer a specific clinical question or concern. However, many mediastinal abnormalities are discovered incidentally, and a CT scan of the chest performed in the routine fashion may be insufficient for the purposes of developing a focused differential diagnosis. Some artifacts induced by technique may simulate pathology, and additional evaluation with electrocardiographic (ECG)-gated cardiac CT scans, MR imaging, or a PET/CT scan with fluorodeoxyglucose (FDG) may add value. An awareness of the potential pitfalls in assessing the mediastinum on imaging studies and effective solutions to mitigate these problematic issues is necessary to ensure an accurate interpretation by radiologists. The

[a] Department of Diagnostic Imaging, Division of Cardiovascular Imaging, The Chaim Sheba Medical Center (affiliated with Tel Aviv University), Derech Sheba 2, Ramat Gan, Israel; [b] Department of Diagnostic Imaging, Division of Thoracic Imaging, University of Texas MD Anderson Cancer Center, 1515 Holcombe Boulevard, Houston, TX 77030, USA; [c] Department of Diagnostic Imaging, Division of Thoracic Imaging, The Chaim Sheba Medical Center (affiliated with Tel Aviv University), Derech Sheba 2, Ramat Gan, Israel
* Corresponding author. The Chaim Sheba Medical Center, Derech Sheba 2, Ramat Gan, Israel.
E-mail address: orly.goitein@sheba.health.gov.il

Radiol Clin N Am 59 (2021) 279–290
https://doi.org/10.1016/j.rcl.2020.11.003

purpose of this review is to highlight and discuss the potential pitfalls in the imaging of the mediastinum.

CYSTIC STRUCTURES

Cystic or fluid-containing structures are commonly encountered in all compartments of the mediastinum, and may represent normal anatomy (such as fluid in the pericardial recesses), cysts (such as thymic or bronchogenic cyst), or cystic neoplasms (such as cystic thymoma). It is important to differentiate cystic neoplasms from benign lesions and normal anatomic structures to ensure appropriate intervention and avoid delays in treatment planning.

In the oncologic setting, one of the most commonly encountered mediastinal anatomic pitfalls relates to pericardial recesses mimicking lymphadenopathy. The pericardium is composed of an outer fibrous component and an inner serous component, which itself has an inner visceral layer, adherent to the heart and great vessels, and an outer parietal layer, which lines the fibrous pericardium. The pericardial space normally contains approximately 15 to 30 mL of fluid between the visceral and parietal layers of the serous pericardium. There are reflections of serous pericardium between the great vessels and at the base of the heart. Physiologic amounts of fluid in these pericardial reflections may vary between imaging studies obtained at different time points. Typical imaging features of fluid-filled pericardial sinuses and recesses include fluid attenuation, contiguity with other pericardial spaces, and no mass effect on adjacent structures. Multiplanar reformations are particularly helpful in demonstrating the relationship between the pericardial recesses and other mediastinal structures, as well as the contiguity with the rest of the pericardium. A distinctive beak-like appearance is seen as fluid in the pericardial recesses drapes over the neighboring mediastinal structures. Of the various pericardial recesses, the high-riding variant of the superior aortic recess extending cephalad into the right paratracheal region constitutes a potential pitfall in oncologic imaging because it can be confused with lymphadenopathy (**Fig. 1**).[2] Owing to its typical appearance, the use of other imaging modalities to confirm pericardial fluid is usually not necessary. However, when in doubt, MR imaging, with its superior contrast resolution, can show the fluid content with high signal intensity on T2-weighted images, low signal intensity on T1-weighted images, and the lack of enhancement after the administration of intravenous contrast. On CT scans, mediastinal lymphadenopathy manifests as soft tissue lesions with lobular margins that may exert a mass effect on the adjacent structures. Depending on the underlying etiology, enlarged lymph nodes may enhance after the administration of intravenous contrast. FDG PET/CT scans can also help to distinguish lymphadenopathy from the pericardial fluid, with the former demonstrating increased FDG uptake in the

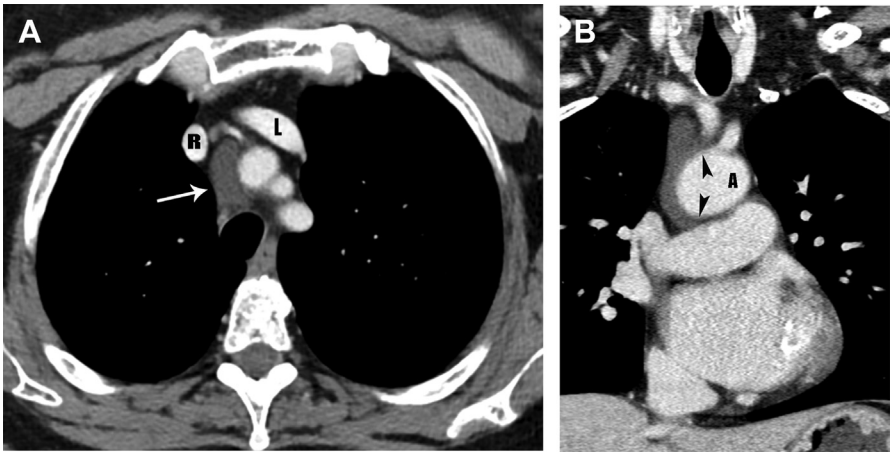

Fig. 1. Superior aortic pericardial recess in a 60-year-old woman. (*A*) A contrast-enhanced axial CT scan of the chest at the level of the right (R) and left (L) brachiocephalic veins demonstrates a homogeneous low attenuation fluid collection (*arrow*) between the right brachiocephalic vein and the innominate artery. (*B*) A coronal reformatted contrast-enhanced CT scan of the chest shows fluid adjacent to the brachiocephalic vessels that is contiguous with the superior aortic recess of the transverse sinus draping over the aorta (A) with a beak-like extension (*arrowheads*).

setting of metastatic disease or active infection or inflammation.

Mediastinal cysts are most commonly encountered in the prevascular compartment, typically within the fat anterior to or lateral to the pericardium. Although surgical series have suggested that cysts represent less than 5% of mediastinal masses, a recent multi-institutional study has shown that mediastinal cysts represent 24% of prevascular mediastinal masses.[3] When a cystic lesion is identified in the prevascular mediastinum, the primary role of the radiologist is to differentiate between a benign cyst such as a thymic or pericardial cyst and a cystic thymoma. Thymic cysts are among most common benign thymic lesions and may be either congenital or acquired. Congenital thymic cysts are unilocular, contain clear fluid, and are found incidentally in asymptomatic patients during the first 2 decades of life.[4,5] Acquired thymic cysts may be multilocular and contain heterogeneous fluid indicating a high protein content owing to infection or hemorrhage. Conditions associated with thymic cysts include thymic neoplasms, radiation therapy, thoracotomy, and chest trauma. Unfortunately, thymic cysts often manifest with internal heterogeneous attenuation that cannot be differentiated from cystic neoplasms on CT imaging alone. A common pitfall in the

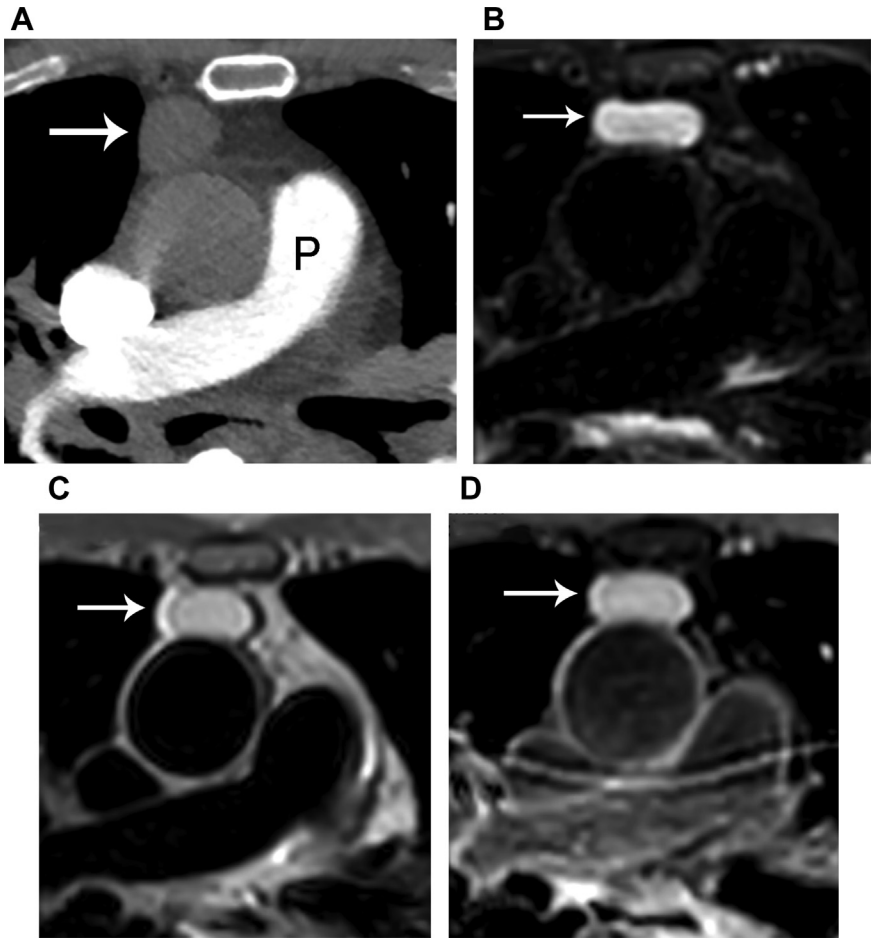

Fig. 2. Thymic cyst in a 68-year-old man with shortness of breath. (*A*) A contrast-enhanced axial CT scan of the chest at the level of the pulmonary trunk (P) demonstrates a homogeneous prevascular mediastinal mass measuring 60 Hounsfield units (*arrow*), suspicious for a solid lesion such as thymoma. (*B*) An axial T2-weighted MR image demonstrates homogeneous high signal intensity without thick septations or nodules (*arrow*). (*C*) An axial T1-weighted MR image demonstrates homogeneous high signal intensity in the lesion (*arrow*). (*D*) An axial T1-weighted MR image obtained after the administration of intravenous gadolinium contrast demonstrates no enhancement, thick septations or nodules, characterizing this lesion as a thymic cyst and differentiating it from a cystic thymoma.

evaluation of benign thymic cysts is misinterpretation as solid masses when their attenuation is higher than expected for fluid (higher than 20 Hounsfield units), which may then lead to unnecessary invasive tissue sampling or surgery.[6] To address this issue, MR imaging can be performed to evaluate these lesions, because it is the optimal imaging modality for distinguishing cystic from solid lesions, identifying cystic and/or necrotic lesion components, characterizing cystic lesions as to the presence of septations and mural nodularity, and distinguishing normal or hyperplastic thymic tissue from neoplasia. Typical characteristics of a thymic cyst on MR imaging include a low signal intensity on T1-weighted images and a uniform high signal intensity on T2-weighted images. After the administration of intravenous contrast, thick, enhancing septations or mural nodularity should be absent (**Fig. 2**). The presence of these findings should raise concern for a thymic malignancy. A high signal intensity on both T1- and T2-weighted images may represent a cystic lesion

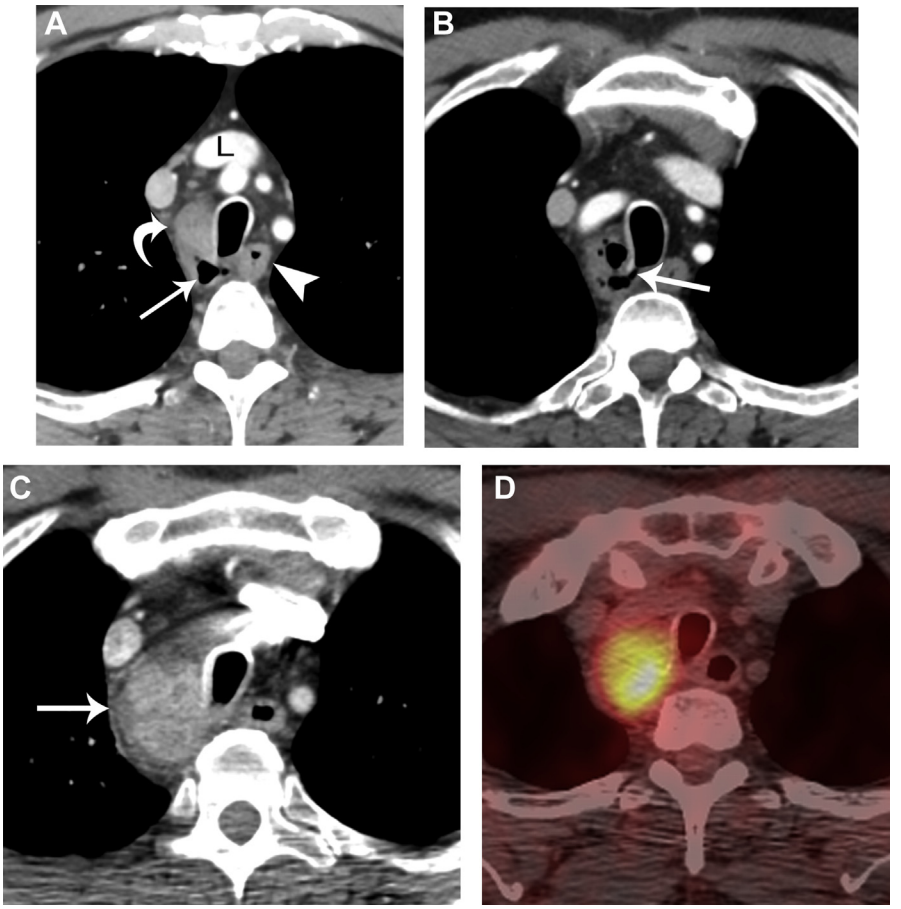

Fig. 3. Tracheal diverticulum in a 52-year-old man with undifferentiated sinonasal carcinoma. (*A*) A contrast-enhanced axial CT scan of the chest at the level of the left brachiocephalic vein (L) demonstrates apparent soft tissue in the right paratracheal region mimicking lymphadenopathy (*curved arrow*). However, upon closer scrutiny, a pocket of air (*straight arrow*) separate from the esophagus (*arrowhead*) is noted. (*B*) A contrast-enhanced axial CT scan of the chest cephalad to the prior image demonstrates that the apparent soft tissue in the right paratracheal region actually represents a fluid-filled tracheal diverticulum. Note the air-filled stalk (*arrow*) connecting this lesion to the tracheal lumen. (*C*) A contrast-enhanced axial CT scan of the chest performed 6 days later shows that the tracheal diverticulum (*arrow*) has increased in size, contains more fluid but less air, and enhances heterogeneously. This CT scan was performed 3 days after bronchoscopy in which the diverticulum was brushed and biopsied. (*D*) A fused axial FDG PET/CT scan performed after the bronchoscopy shows increased FDG uptake in the paratracheal lesion that could be misinterpreted as a neoplasm. However, this uptake was due to inflammation from a recent invasive procedure. The tracheal diverticulum decreased in size and FDG avidity on subsequent studies (not shown).

complicated by hemorrhage or infection. To avoid misinterpretation of a thymic malignancy as benign, it is important to pay close attention to the T1-weighted images after intravenous contrast administration, because enhancement is noted in the early dynamic phase in 90% of tumors, and the remaining 10% show enhancement on delayed T1-weighted images.[7]

Tracheal diverticula are outpouchings from the tracheal wall that are lined with ciliated columnar epithelium. They are usually 5 to 25 mm in size. Although tracheal diverticula are connected to the airways by definition, the connecting stalk is frequently below the spatial resolution of a CT scan. These diverticula characteristically present as small air bubbles along the right posterolateral wall of the upper trachea (at the level of T1–T3). However, tracheal diverticula may contain fluid, particularly in patients with cystic fibrosis.[8] Depending on the protein content of the fluid,

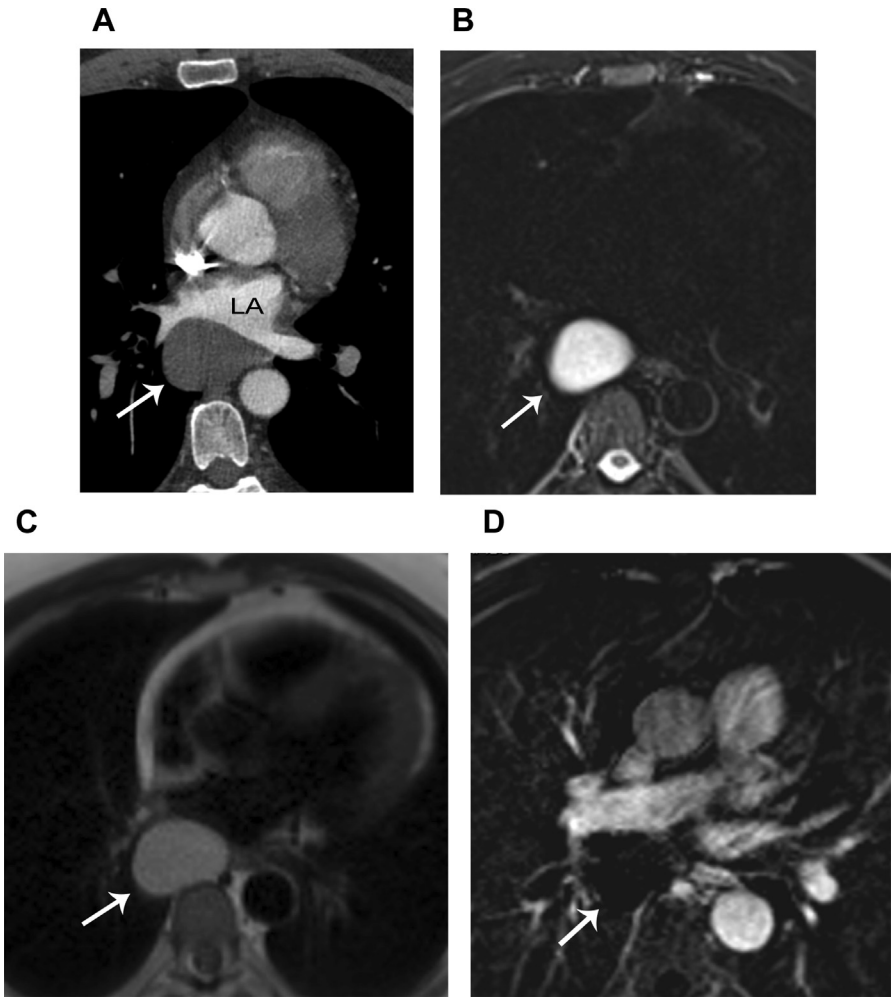

Fig. 4. A bronchogenic cyst in a 50-year-old woman with persistent cough. (*A*) A contrast-enhanced axial CT scan of the chest at the level of the left atrium (LA) demonstrates a homogeneous low attenuation (38 Hounsfield units) mass (*arrow*) in the visceral mediastinum compressing the left atrium. On CT scan, cysts with hemorrhage or proteinaceous material may demonstrate density similar to soft tissue and can be misinterpreted as solid lesions. (*B*) An axial T2-weighted MR image demonstrates homogeneous high signal intensity in the lesion (*arrow*), consistent with a cyst. (*C*) An axial T1-weighted MR image demonstrates homogeneous high signal intensity relative to muscle (*arrow*). The high signal intensity on both T1- and T2-weighted images confirms the proteinaceous cyst content. (*D*) A subtracted fat-suppressed axial T1-weighted MR image after the administration of intravenous gadolinium contrast demonstrates no enhancement of either the lesion or its wall (*arrow*) and no nodules. MR imaging is the optimal imaging modality for distinguishing cystic from solid lesions, identifying cystic and/or necrotic lesion components, and characterizing cystic lesions as to the presence of septations and mural nodularity.

tracheal diverticula may be misinterpreted as a cyst or a lymph node, which carries implications in the oncologic setting (**Fig. 3**). Although most patients are asymptomatic, some may rarely present with cough owing to pulmonary aspiration or pneumonia, because the diverticula may serve as a reservoir for food residue or secretions.[8,9]

Bronchogenic cysts result from abnormal budding of the primitive foregut, which also gives rise to the tracheobronchial tree, during embryologic development. These benign lesions may arise from any mediastinal compartment, but typically occur in the visceral compartment near the carina or, less commonly, the right paratracheal region. Histologically, bronchogenic cysts are lined by respiratory epithelium and contain a thick mucoid material. Bronchogenic cysts can grow substantially in size without causing symptoms; however, patients may report symptoms when adjacent mediastinal structures are compressed. Bronchogenic cysts typically manifest as well-defined lesions composed of simple fluid. However, when CT attenuation of fluid with a high protein content approaches that of soft tissue, bronchogenic cysts may be misinterpreted as neoplasms. MR imaging adds value by demonstrating the cystic nature with a high signal intensity on T2-weighted images. The signal intensity on T1-weighted images varies depending on the cyst contents (**Fig. 4**).[5]

A Zenker's diverticulum (pharyngeal pouch) is a typical pulsion diverticulum that represents an acquired sac-like posterior outpouching of the hypopharynx proximal to the upper esophageal sphincter through a *locus minoris resistentiae* in the muscular layer (Killian dehiscence). The typical location is at the C5 to C6 level, although extension into the mediastinum may be seen when large.[10,11] Zenker's diverticula usually present in the seventh and eighth decades of life, with a 1.5 times male predominance. Their true prevalence is probably underestimated, because many diverticula remain clinically silent. Although fluoroscopic esophagram is often used to diagnose Zenker's diverticula owing to the dynamic nature of the modality, they may be incidentally detected on a CT scan (**Fig. 5**).

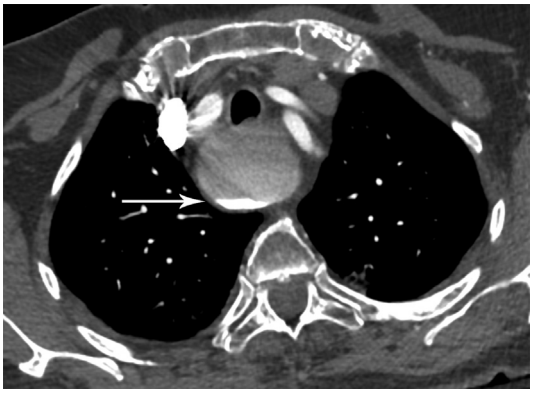

Fig. 5. A large Zenker's diverticulum in an 81-year-old woman undergoing CT imaging for pulmonary embolism. A contrast-enhanced axial CT scan of the chest shows a fluid–fluid level (*arrow*) within a large retrotracheal cystic lesion, representing a large Zenker's diverticulum. The layering effect reflects the different attenuation coefficients of various esophageal contents. The content of a Zenker's diverticulum may at times be of high attenuation mimicking intravenous contrast. This should not be mistaken for hemorrhage. When in doubt, a repeat chest CT scan without intravenous contrast may be helpful.

VASCULAR STRUCTURES

A variety of normal vascular structures may be misinterpreted as pathology in specific circumstances. For example, valves in the azygos and hemiazygos veins may accumulate intravenous contrast and mimic calcified lymph nodes on a CT scan (**Fig. 6**).[12] Flow-related artifacts owing to the mixing of unenhanced and enhanced blood may be mistaken for an intravascular filling defect or thrombus. Obtaining a delayed scan in the venous phase may help to avoid this potential pitfall (**Fig. 7**). Pulmonary artery motion and inspirational flow-related artifacts may simulate a filling defect or dissection. Obtaining a delayed scan in the venous phase or repeating the scan with

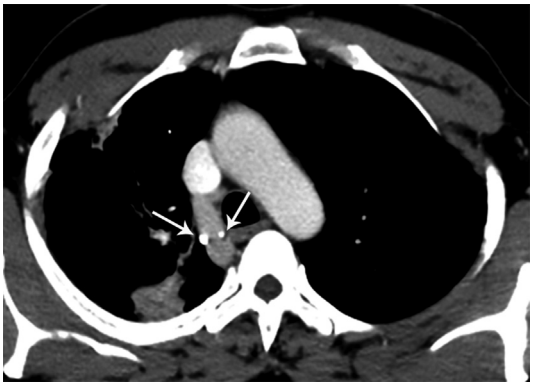

Fig. 6. Azygos arch valves in a 68-year-old man with tuberculosis in the right upper lobe. A contrast-enhanced axial CT scan of the chest demonstrates the reflux of intravenous contrast into the azygos vein, lodged within the valves (*arrows*). Knowledge of the typical appearance and location of the azygos arch valves is important in avoiding misinterpretation as calcified lymph nodes, calcified thrombus or a foreign body.

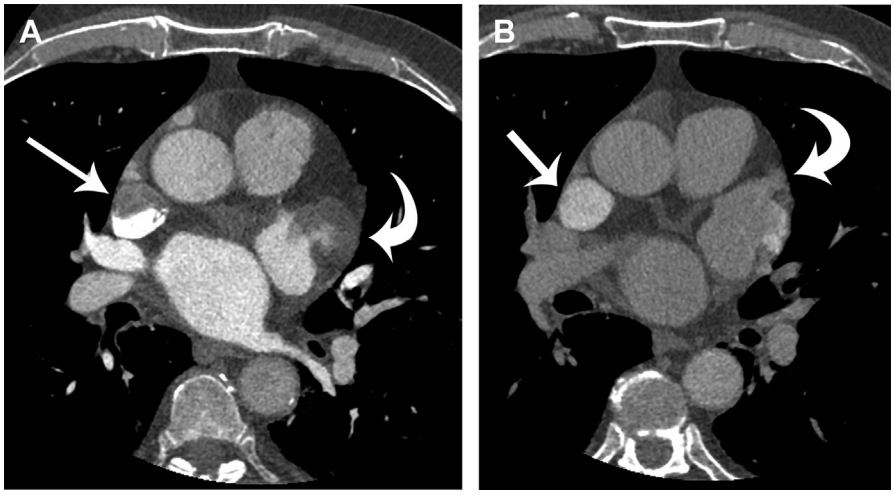

Fig. 7. Flow artifact in a 70-year-old man with atrial fibrillation undergoing imaging evaluation for thrombus in the left atrial appendage. (*A*) A contrast-enhanced axial CT scan of the heart in the arterial phase demonstrates a low attenuation focus along the anterior aspect of the superior vena cava (*arrow*). This flow artifact is caused by the mixing and volume averaging of unenhanced blood with contrast-enhanced blood on an arterial phase CT scan. Slow flow within the trabeculated left atrial appendage simulates a thrombus (*curved arrow*). (*B*) A contrast-enhanced axial CT scan of the heart in the delayed phase shows a more homogenous appearance of the superior vena cava (*arrow*) and the left atrial appendage (*curved arrow*). Better mixing of contrast with the blood on delayed phase confirms the absence of thrombus.

ECG gating are solutions to address these issues (**Fig. 8**).[13,14]

CARDIAC STRUCTURES

Technical advances in CT technology, with faster rotation times and shorter scan durations, lead to better delineation of cardiac structures with less motion artifacts even in the absence of ECG gating. Familiarity with age-related cardiac changes, flow artifacts, and anatomic variations is useful to avoid misinterpretation as cardiac pathology.

Aortic wall motion during the cardiac cycle may result in curvilinear artifacts that characteristically appear in proximity to the aortic root, where the cardiac motion is most prominent. ECG gating increases the diagnostic accuracy and substantially decrease motion artifacts in the aortic root and proximal ascending aorta without increasing radiation exposure (**Fig. 9**).[15–17]

The left atrial appendage (LAA) anatomy is highly variable and complex with multiple prominent trabeculations and thin walls. In patients with atrial fibrillation, slow flow, blood stasis, and thrombus formation often occur and can be challenging to diagnose. Recently, interest in LAA imaging has increased owing to the need to

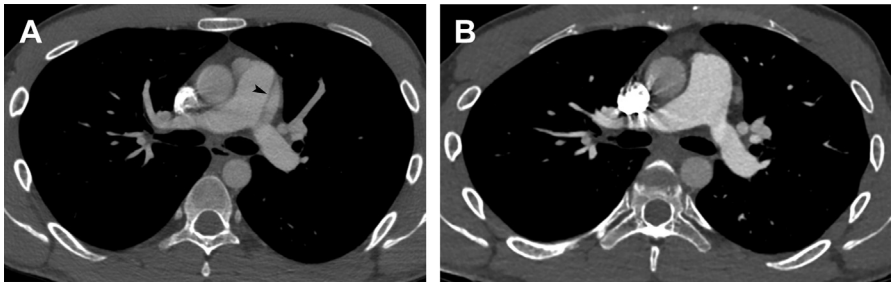

Fig. 8. Cardiac motion artifact in a 48-year-old man undergoing imaging after a traumatic injury. (*A*) A contrast-enhanced axial non–ECG-gated CT scan at the level of the pulmonary trunk demonstrates a linear low attenuation band (*arrowhead*) along the long axis of the pulmonary trunk suspicious for pulmonary artery dissection. (*B*) A contrast-enhanced axial ECG-gated CT scan performed the following day demonstrates a normal appearance of the pulmonary trunk. ECG gating is useful in resolving cardiac motion artifact.

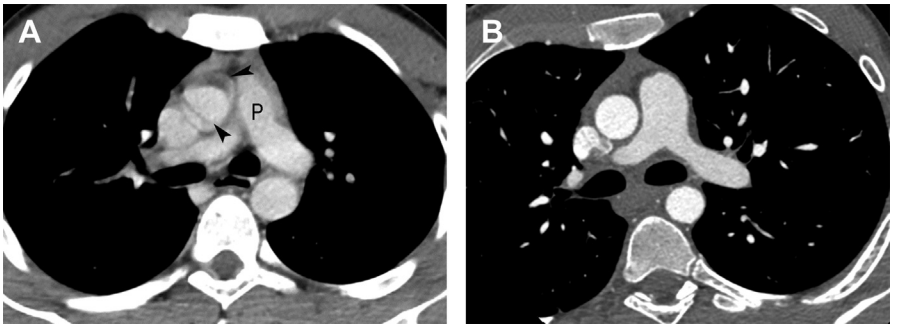

Fig. 9. Cardiac motion artifact in a 20-year-old man imaged after a motor vehicle collision. (*A*) A contrast-enhanced axial non–ECG-gated CT scan at the level of the pulmonary trunk (P) demonstrates motion artifact (*arrowheads*) in the ascending aorta mimicking aortic injury. (*B*) A contrast-enhanced axial ECG-gated CT scan subsequently performed demonstrates a normal appearance of the ascending aorta. Awareness of the potential pitfall of cardiac motion artifact on the appearance of cardiovascular structures on non-ECG studies and the need to perform ECG gating when appropriate is important.

make clinical decisions regarding antithrombotic treatment: cardioversion, pulmonary vein ablation and LAA occluder insertion. The accurate detection of an LAA thrombus is important because this entity is the main cause of stroke in nonvalvular atrial fibrillation. Documenting LAA thrombus is crucial in obviating the need for further LAA imaging before cardioversion LAA occlusion or pulmonary vein ablation. The approach to the evaluation of the LAA includes delayed imaging with or without ECG gating, prone positioning, and dual energy or dual source imaging. Delayed LAA imaging shows the value of sensitivity, specificity, positive predictive value, and negative predictive value of 100%, 99%, 92%, and 100%, respectively, in the detection of thrombus (**Fig. 10**).[18,19]

Congenital left ventricular clefts, diverticula, and aneurysms are usually asymptomatic and discovered incidentally during cross-sectional imaging evaluation. Myocardial crypts or clefts are slit-like invaginations within the left ventricular myocardium, observed mostly between the insertion points between the left and right

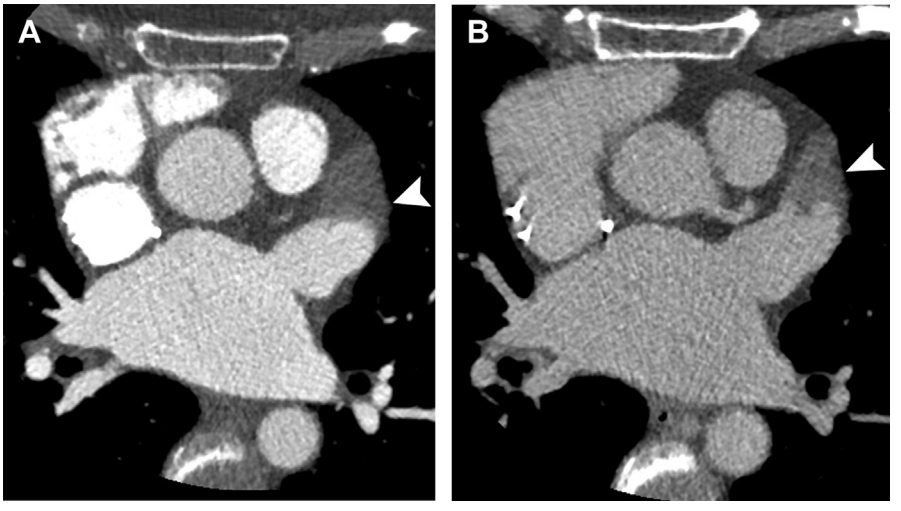

Fig. 10. A 68-year-old man undergoing imaging evaluation before left atrial appendage occlusion. (*A*) A contrast-enhanced axial ECG-gated CT scan in the arterial phase demonstrates an apparent filling defect in the nondependent portion of the LAA (*arrowhead*), raising the question of thrombus. This appearance is commonly seen in early phase imaging before the unenhanced blood and contrast enhanced blood have had a chance to mix homogeneously. (*B*) A contrast-enhanced axial ECG-gated CT scan in the venous phase (40-second delay) demonstrates that the LAA filling defect (*arrowhead*) persists confirming the diagnosis of thrombus.

ventricles. Crypts are defined as blood-filled invaginations penetrating more than 50% of the myocardial thickness. As CT technological advances lead to greater temporal and spatial resolution, such cardiac findings are visualized more frequently. Myocardial crypts have been reported in normal subjects, hypertrophic cardiomyopathy, aortic stenosis, and hypertension with a reported prevalence of 4% to 9%. Awareness of this entity is essential to avoid misinterpretation and to correlate with relevant underlying clinical conditions (**Fig. 11**).[18,20,21]

FAT-CONTAINING STRUCTURES

Fat necrosis abutting the heart, also known as pericardial, epipericardial, or mediastinal fat necrosis, is an uncommon, benign condition of unclear etiology. It is typically located in the cardiophrenic angle, more often on the left. A CT scan usually demonstrates a well-circumscribed round or ovoid mass-like lesion with soft tissue or fat attenuation and adjacent inflammatory changes. On FDG PET/CT scanning, fat necrosis may show increased FDG uptake if imaged during the inflammatory phase. Two clinical scenarios highlight the importance in recognizing this entity. In the symptomatic patient, the detection of fat necrosis as a cause of chest pain aids in avoiding unnecessary additional investigation or invasive procedures. In the asymptomatic patient, awareness of this benign entity is important to avoid misinterpretation as malignancy or lymphadenopathy. When first reported in the literature, patients with fat necrosis had undergone surgical exploration and resection of these lesions. Because epicardial fat necrosis is benign and self-limiting, the current treatment is conservative, with anti-inflammatory agents, and resolution of symptoms

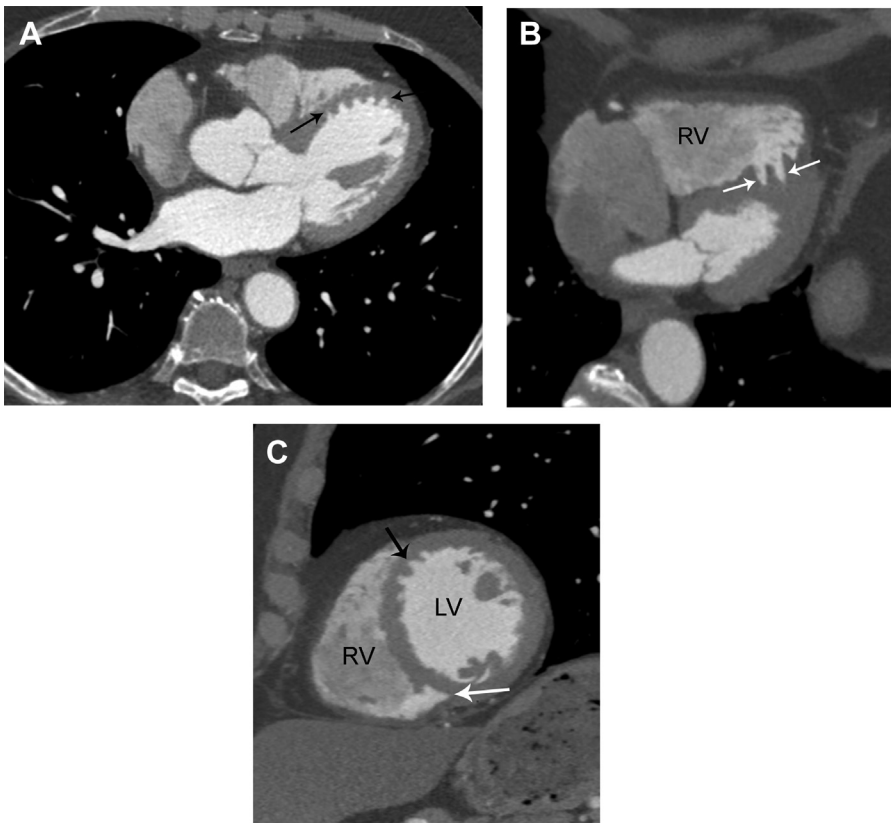

Fig. 11. Myocardial crypts in a 65-year-old woman with shortness of breath undergoing evaluation for a pulmonary embolism. (*A*) A contrast-enhanced axial ECG-gated CT scan demonstrates crypts along the left ventricular wall (*black arrows*). (*B*) A contrast-enhanced axial ECG-gated CT scan shows normal right ventricular (RV) myocardial trabeculations (*white arrows*) in the interventricular septum. (*C*)A contrast-enhanced short axis ECG-gated CT scan demonstrates true crypts (*black arrow*) in the left ventricular septum and normal anatomy of the RV wall trabeculations (*white arrow*). In the normal heart, the RV wall is trabeculated, whereas the left ventricular wall is usually smooth.

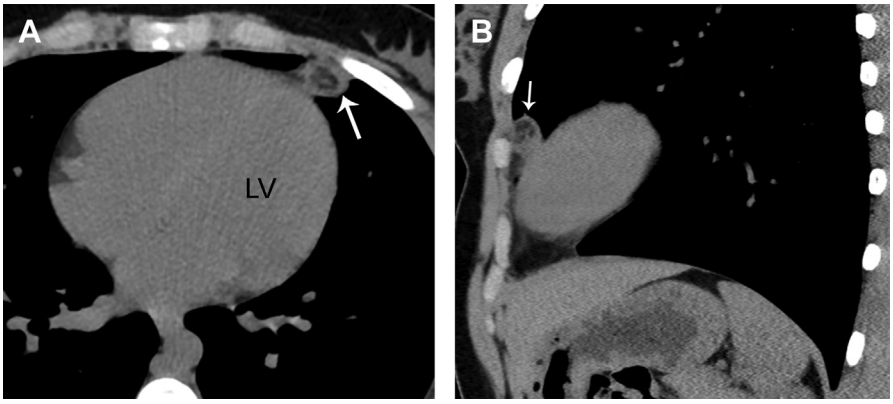

Fig. 12. Pericardial and epipericardial fat necrosis in a 20-year-old woman who presented to the emergency department with acute chest pain. (*A*) An unenhanced axial CT scan of the chest demonstrates an oval mass (*arrow*) abutting the left ventricle (LV). There is a soft tissue ring surrounding a fat-containing center and associated mild stranding of the adjacent mediastinal fat. These imaging findings are characteristic of pericardial and epipericardial fat necrosis. (*B*) An unenhanced sagittal reformation demonstrates the oval mass (*arrow*) with stranding of the adjacent mediastinal fat.

within 3 to 4 days after treatment initiation. Knowledge of this entity is important to obtain a correct diagnosis and avoid unnecessary surgical interventions (**Fig. 12**).[22,23]

Brown adipose tissue or fat plays an important role in cold-induced and diet-induced thermogenesis. Brown fat has glucose transporters and can show physiologic FDG uptake, more commonly seen in cold weather and younger individuals. It is typically seen in the supraclavicular regions in a symmetric and elongated distribution on a FDG PET/CT scan. However, when encountered in the mediastinum, it can be confused with lymphadenopathy on staging or on follow-up FDG PET/CT imaging. Hypermetabolic brown fat in the mediastinum has been reported in 1.8% of oncologic patients, with locations in the paratracheal, paraesophageal, prevascular, and pericardial regions; interatrial septum; and azygoesophageal recess.[24] Knowledge of this potential pitfall is imperative to avoid misinterpretation as nodal disease and lead to errors in the staging and follow-up of oncologic patients. Careful inspection of the CT images to localize the foci of FDG avidity

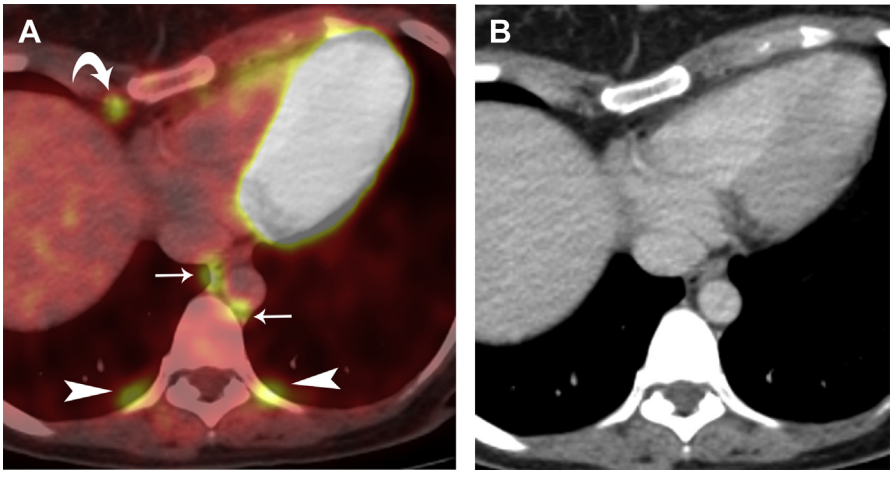

Fig. 13. Brown adipose tissue in a 34-year-old woman undergoing follow-up imaging related to melanoma. (*A*) A fused axial FDG PET/CT scan shows foci of increased FDG uptake in the prevascular mediastinum (*curved arrow*), adjacent to the azygous and hemiazygous veins (*arrows*), and in the bilateral paraspinal regions (*arrowheads*). (*B*) A contrast-enhanced axial CT scan of the chest localizes these foci of increased FDG uptake to areas of fat. No lymph nodes were identified in these regions. Deposits of brown adipose tissue can show increased FDG uptake on PET/CT scans owing to cold stimulus.

to areas of fat aids in accurate interpretation (**Fig. 13**).

SUMMARY

Potential pitfalls that may be encountered in imaging of the mediastinum include normal structures and variants, various artifacts, and benign lesions that may mimic malignant neoplasms, and may involve cystic, vascular, cardiac, and fat-containing anatomic regions. Familiarity with the variety of potential pitfalls is important to avoid misinterpretation, which may alter patient management and lead to unnecessary investigation and/or procedures.

CLINICS CARE POINTS

- Advances in multidetector CT technology allow for better delineation of mediastinal structures but also results in the routine visualization of normal anatomic structures and anatomic variants which can be confused with pathology, as well as benign lesions that may mimic malignant neoplasms.
- If a mediastinal mass is suspected to be cystic, MR imaging adds value by demonstrating its fluid content and is helpful to differentiate benign from malignant disease.
- In the symptomatic patient, imaging detection of fat necrosis as a cause of chest pain aids in avoiding unnecessary additional investigation or invasive procedures.

DISCLOSURE

Nothing to disclose for all authors.

REFERENCES

1. Tomiyama N, Honda O, Tsubamoto M, et al. Anterior mediastinal tumors: diagnostic accuracy of CT and MRI. Eur J Radiol 2009;69(2):280–8.
2. Shroff GS, Viswanathan C, Godoy MC, et al. Pitfalls in oncologic imaging: pericardial recesses mimicking adenopathy. Semin Roentgenol 2015;50(3):235–40.
3. Roden AC, Fang W, Shen Y, et al. Distribution of mediastinal lesions across multi-institutional, international, radiology databases. J Thorac Oncol 2020;15(4):568–79.
4. Jeung MY, Gasser B, Gangi A, et al. Imaging of cystic masses of the mediastinum. Radiographics 2002;22 Spec No:S79–93.
5. Takeda S, Miyoshi S, Minami M, et al. Clinical spectrum of mediastinal cysts. Chest 2003;124(1):125–32.
6. Ackman JB, Verzosa S, Kovach AE, et al. High rate of unnecessary thymectomy and its cause. Can computed tomography distinguish thymoma, lymphoma, thymic hyperplasia, and thymic cysts? Eur J Radiol 2015;84(3):524–33.
7. Hammer MM, Barile M, Bryson W, et al. Errors in interpretation of magnetic resonance imaging for thymic lesions. J Thorac Imaging 2019;34(6):351–5.
8. Gayer G. Tracheal diverticula. Semin Ultrasound CT MR 2016;37(3):190–5.
9. Gayer G, Sarouk I, Kanaany N, et al. Tracheal diverticula in cystic fibrosis-A potentially important underreported finding on chest CT. J Cyst Fibros 2016;15(4):503–9.
10. Bizzotto A, Iacopini F, Landi R, et al. Zenker's diverticulum: exploring treatment options. Acta Otorhinolaryngol Ital 2013;33(4):219–29.
11. Siddiq MA, Sood S, Strachan D. Pharyngeal pouch (Zenker's diverticulum). Postgrad Med J 2001;77(910):506–11.
12. Yeh BM, Coakley FV, Sanchez HC, et al. Azygos arch valves: prevalence and appearance at contrast-enhanced CT. Radiology 2004;230(1):111–5.
13. Ardley ND, Lau KK, Buchan K, et al. Effects of electrocardiogram gating on CT pulmonary angiography image quality. J Med Imaging Radiat Oncol 2014;58(3):303–11.
14. Gosselin MV, Rassner UA, Thieszen SL, et al. Contrast dynamics during CT pulmonary angiogram: analysis of an inspiration associated artifact. J Thorac Imaging 2004;19(1):1–7.
15. Bolen MA, Popovic ZB, Tandon N, et al. Image quality, contrast enhancement, and radiation dose of ECG-triggered high-pitch CT versus non-ECG-triggered standard-pitch CT of the thoracoabdominal aorta. AJR Am J Roentgenol 2012;198(4):931–8.
16. Schernthaner RE, Stadler A, Beitzke D, et al. Dose modulated retrospective ECG-gated versus non-gated 64-row CT angiography of the aorta at the same radiation dose: comparison of motion artifacts, diagnostic confidence and signal-to-noise-ratios. Eur J Radiol 2012;81(4):e585–90.
17. Stein E, Mueller GC, Sundaram B. Thoracic aorta (multidetector computed tomography and magnetic resonance evaluation). Radiol Clin North Am 2014;52(1):195–217.
18. Budoff MJ, Shittu A, Hacioglu Y, et al. Comparison of transesophageal echocardiography versus computed tomography for detection of left atrial appendage filling defect (thrombus). Am J Cardiol 2014;113(1):173–7.
19. Romero J, Husain SA, Kelesidis I, et al. Detection of left atrial appendage thrombus by cardiac computed tomography in patients with atrial fibrillation: a meta-analysis. Circ Cardiovasc Imaging 2013;6(2):185–94.
20. Maron MS, Rowin EJ, Lin D, et al. Prevalence and clinical profile of myocardial crypts in hypertrophic cardiomyopathy. Circ Cardiovasc Imaging 2012;5(4):441–7.
21. Petryka J, Baksi AJ, Prasad SK, et al. Prevalence of inferobasal myocardial crypts among

patients referred for cardiovascular magnetic resonance. Circ Cardiovasc Imaging 2014;7(2):259–64.
22. Gayer G. Mediastinal (Epipericardial) fat necrosis: an overlooked and little known cause of acute chest pain mimicking acute coronary syndrome. Semin Ultrasound CT MR 2017;38(6):629–33.
23. Giassi KS, Costa AN, Bachion GH, et al. Epipericardial fat necrosis: who should be a candidate? AJR Am J Roentgenol 2016;207(4):773–7.
24. Truong MT, Erasmus JJ, Munden RF, et al. Focal FDG uptake in mediastinal brown fat mimicking malignancy: a potential pitfall resolved on PET/CT. AJR Am J Roentgenol 2004;183(4):1127–32.